



Stable isotope characterisation of recent aragonite travertine deposits associated with the Fitero thermal waters (Spain)

Mónica Blasco¹ · Luis F. Auqué¹ · María J. Gimeno¹ · María P. Asta² · Juan Mandado¹

Received: 19 August 2019 / Accepted: 8 February 2020 / Published online: 27 February 2020
© Geologische Vereinigung e.V. (GV) 2020

Abstract

The travertines of the Fitero thermal springs, with more than 98% of aragonite in most of the samples, are studied in this paper. The main objective is to improve the general understanding of aragonite precipitation, since the deposits of almost pure aragonite are very scarce. This study presents a complete mineralogical and isotopic characterisation, including the evaluation of the $\delta^{18}\text{O}$ and $\delta^{13}\text{C}$ fractionation during precipitation, as valuable information for paleoclimate and paleoenvironmental studies. Samples of a laminated travertine deposit constituted by almost pure aragonite were taken from a pipe discharging water at 40 °C. Waters suffered an important CO_2 outgassing, as suggested by the geochemical calculations and the $\delta^{13}\text{C}$ values of travertines and waters. This outgassing triggers the oversaturation and precipitation of carbonate phases. Temperature seems to be the main factor controlling the precipitation of aragonite or calcite, as checked by studying another travertine sample with higher calcite content. Various $\delta^{18}\text{O}$ isotope fractionation equations for aragonite and calcite were used. The results indicate that precipitation took place close to equilibrium according to some of these equations. The fact that the equilibrium is maintained in a natural system with an important CO_2 loss is surprising. However, it can be explained by an HCO_3^- –water oxygen isotopic equilibrium and a direct transfer of the HCO_3^- isotope signal to the carbonate without fractionation due to the fast CO_2 loss and precipitation. Finally, considering other natural aragonite samples, a fractionation equation is defined for natural aragonite in the temperature range between 23 and 80 °C.

Keywords Geothermal system · Travertine · Aragonite · Stable isotope · Isotope equilibrium

Introduction

The Fitero thermal springs (Navarra region, Spain) are quite well known, and their waters are used in two spas in the village for their medicinal and therapeutic properties. They have been studied by different authors (e.g., Auqué et al. 1988, 1989; Fernández et al. 1988; Coloma et al. 1995, 1996, 1997a, 1998; Blasco et al. 2019) obtaining the temperature in the deep reservoir, a complete chemical and isotopic characterisation of the hydrogeochemical system,

and a good knowledge of the main processes controlling the evolution of the waters.

Despite this broad characterisation of the thermal waters, the travertines precipitating from them are still almost unstudied. That is why, the first objective of this research is the in-depth study of these travertines¹. The fact that some of the Fitero travertines consist of almost pure aragonite (with less than 2% of calcite) makes this system even more interesting, because there are very few studies about pure or almost pure aragonite travertines or tufas, as most of them are mixtures of calcite and aragonite and they are studied as a whole. Therefore, the mineralogical and isotopic study of the aragonite travertine will help to improve the general understanding of the aragonite precipitation process. Additionally, the study of another more calcite-rich travertine (60% of calcite), precipitated from the same thermal waters,

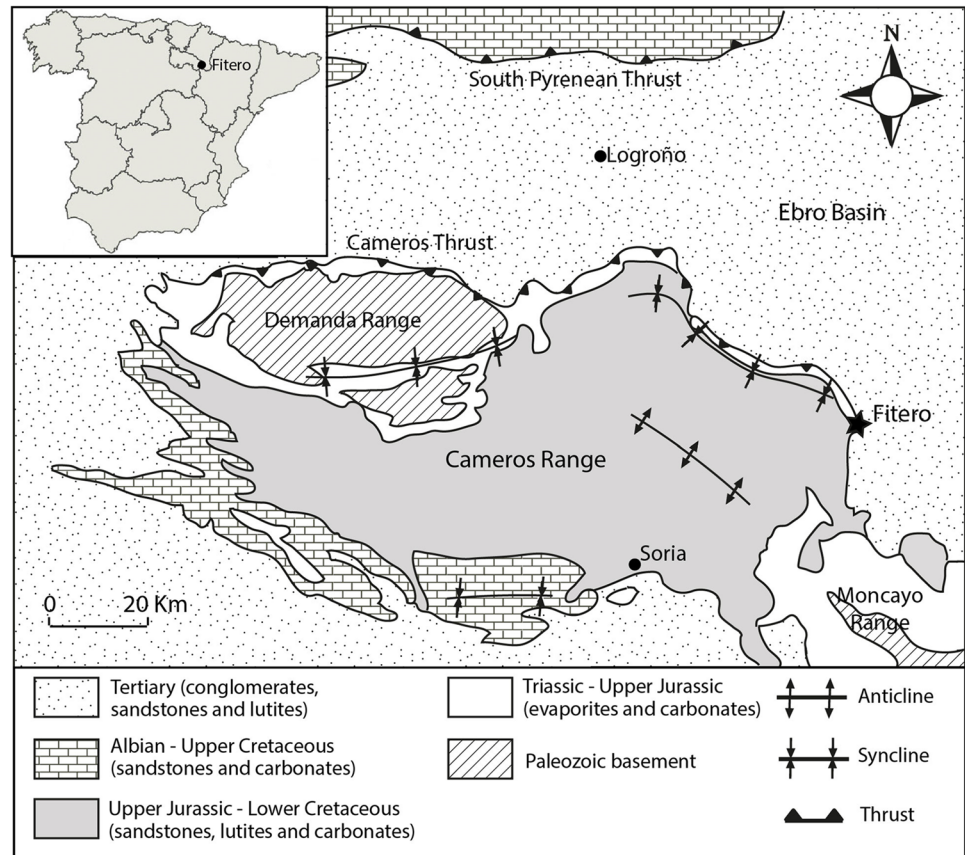
¹ The terminology that will be used here is the one proposed by Ford and Pedley (1996) in which the term travertine is used to refer to the carbonates precipitated from thermal (hot) waters, while the term tufa is reserved for the carbonates precipitated from cold waters (e.g. rivers).

✉ Mónica Blasco
monicabc@unizar.es

¹ Geochemical Modelling Group, Petrology and Geochemistry Area, Earth Sciences Department, University of Zaragoza, C/Pedro Cerbuna 12, 50009 Zaragoza, Spain

² Institut Des Ciencias de La Terre (ISTerre), Université Grenoble Alpes, CNRS, 1381 Rue de la Piscine, 38610 Gières, France

Fig. 1 Location of the Fitero geothermal springs and geological map of the area (modified from Blasco et al. 2018)



will serve for comparative purposes and to evaluate the main controlling factors responsible for the precipitating mineral phases.

The thermal springs in the Fitero spa are currently controlled for their use in the balneotherapeutic facilities and the travertines studied here are generated inside water discharging pipes; however, their study will still be useful for the objectives of this work as it has already been done by other authors such as Asta et al. (2017) in travertines collected in the facilities of other spas, Rodríguez-Berriguete et al. (2018) in tufas precipitated in a pipe used for irrigation or Arenas et al. (2018) in a tufa generated in a pipe that diverted water from a river.

The relevance of the isotope characterisation of these solids lies on the fact that the stable $\delta^{18}\text{O}$ isotope signature of travertines, tufas, and speleothems precipitated under equilibrium conditions depends on the temperature and, therefore, it can be used for paleoenvironmental and paleoclimatic reconstructions (e.g., Ford and Pedley 1996; Fouke et al. 2000; Garnett et al. 2004; Pentecost 2005; Andrews 2006; Liu et al. 2006, 2010; Kele et al. 2008, 2011; Pedley 2009; Jones and Renaut 2010; Osácar et al. 2013, 2016; Capezzoli et al. 2014; Lachniet 2015) using empirical and experimental temperature-dependant equations assumed to represent the isotopic equilibrium between travertine and water.

However, the paleothermometrical interpretation of the stable isotopes in carbonates is not always straightforward due to several reasons: (1) the isotopic signature of the old travertines parental water is unknown; (2) the equilibrium is not always attained, or maintained, during the travertine precipitation due to kinetic isotope effects related to CO_2 outgassing and high precipitation rates (e.g., Fouke et al. 2000; Kele et al. 2008, 2011); and (3) the representativeness of those equations with respect to the real equilibrium is not always guaranteed (e.g., Kele et al. 2015; Lachniet 2015). All these difficulties make the study of actively precipitating travertines an interesting subject that will help to interpret the isotope composition in old travertines.

Geological and hydrological setting

The Fitero thermal waters emerge in the NW part of the Iberian Chain, in the contact between the Cameros Range and the Tertiary Ebro Basin (an NW–SW thrust; Fig. 1; Coloma et al. 1997a; Sánchez and Coloma 1998). The Cameros Range consists mainly of Mesozoic rocks which are divided in three different sequences: (1) the pre-rift sequence represented by Triassic and marine Jurassic rocks (with the classic formations of the Iberian Chain; Goy et al. 1976; Coloma

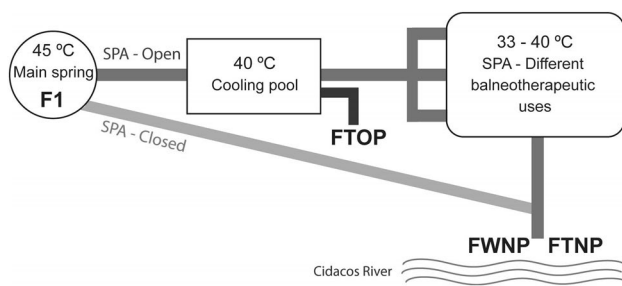


Fig. 2 Idealised scheme of the Spa facilities showing the location where the different samples were taken

1998; Gil et al. 2002); (2) the syn-rift sequence deposited during a rifting process initiated at the end of Jurassic and constituted by fluvial and lacustrine sediments from Upper Jurassic (Tithonian) to Upper Cretaceous (Lower Albian) (Mas et al. 1993; Coloma 1998; Gil et al. 2002); and (3) the post-rift sequence which is constituted by the Upper Cretaceous carbonates and sandstones and the Later Cretaceous carbonate rocks (Gil et al. 2002). Finally, during the Tertiary, a tectonic inversion created the Cameros Range and the Ebro basin (Coloma 1998; Gil et al. 2002).

The reservoir of the Fitero thermal waters is located in the carbonates of the pre-rift sequence (see Blasco et al. 2018 or Blasco et al. 2019 for more details about the geology and hydrogeology of this area) from which they ascend to the surface through the Cameros thrust. The springs are associated with the Keuper facies and the Lower Jurassic carbonates (Auqué et al. 1988; Coloma et al. 1996; Coloma 1998), their flow rate is about 50 L/s, and the spring temperature is close to 50 °C (Coloma et al. 1995, 1997b, 1998; Sánchez and Coloma 1998).

Methodology

Field sampling

A sample of the thermal water, F1 (at 45.5 °C), was taken in a spring inside the Becquer spa, in Fitero (Navarra, Spain). For its use in the spa, this water is cooled down to 40 °C in a pool from where it is distributed to the different balneotherapeutic facilities at that temperature or even lower.

A travertine sample named FTOP (Fitero Travertine Old Pipe) was taken in an old pipe that drained the thermal water from the cooling pool in the moments of exceeding water (Fig. 2) and, therefore, the water circulating through it was at a constant temperature of 40 °C. The diameter of this old pipe was about 30 cm and the inclination close to 30° with a height difference of 20 m from the pool to the exit point of the pipe. The travertine precipitation was so important that the pipe was almost completely clogged and it had to

be removed, which gave the chance to get the solids sample but not the directly related water.

Another travertine sample, FTNP (Fitero Travertine New Pipe), was taken at the end of a currently active pipe that collects the final discharge water from the spa and pours it into the Cidacos river (Fig. 2). The temperature of this discharge water oscillates between 33 and 40 °C during the spa operation times (depending on the different balneotherapeutic uses) and, when the spa is closed, it comes directly from the main spring undergoing a natural cooling. As this is an active pipe, a sample of the discharging water, FWNP (Fitero Water New Pipe), was taken at the same time as the travertine FTNP when the spa was closed and the measured water temperature was 33 °C.

Analytical determinations

Temperature, pH, and electrical conductivity were measured in situ and separate samples for cation, anion, and isotopic analyses were taken. The anions were analysed in the Geochemistry Laboratory of the Department of Earth Sciences at the University of Zaragoza: alkalinity was determined by titration, sulphate by colorimetry, and chloride and fluoride by selective electrodes. The major cations were analysed by ICP-OES, the minor cations by ICP-MS, and $\delta^{18}\text{O}$ and $\delta^2\text{H}$ in water, and $\delta^{13}\text{C}$ in the dissolved inorganic carbon, were analysed by CF-IRMS, all in the Scientific and Technological Centre of the University of Barcelona (Spain). The average analytical error was estimated < 5% for alkalinity, chloride, sulphate, and sodium, < 0.6% for magnesium and potassium and < 0.1% for silica, strontium, and iron. For the isotopes, the analytical precision is 0.2‰ for $\delta^{18}\text{O}$, 1‰ for $\delta^2\text{H}$ and 0.3‰ for $\delta^{13}\text{C}$. More details about the sampling and analytical procedures can be found in Blasco et al. (2018).

Petrographical and mineralogical observations of the travertines were conducted using petrographic microscope on polished thin sections, and field-emission scanning electron microscope (FESEM, using a Carl Zeiss MERLIN™) on carbon-coated samples. Thin sections preparation and FESEM analyses were performed at the facilities of the Research Support Services at the University of Zaragoza.

A small drill was used to separate the material from the different layers in the travertine deposits and the obtained solid samples were crushed in a steel jaw crusher and ground to a size fraction below 60 μm . The bulk mineralogical composition was determined by X-ray diffractometry (XRD) using a PANalytical X'Pert PRO MPD powder diffractometer in Bragg–Brentano $\theta/2\theta$ geometry of 240 mm of radius with a focalising Ge (111) primary monochromator, a X'Celerator detector and using $\text{CuK}\alpha_1$ radiation: $\lambda = 1.5406 \text{ \AA}$ at the X-Ray Diffraction Unit in the Scientific and Technological Centre of the University of Barcelona. Semi-quantitative phase analysis of the identified crystalline

phases was performed by the Rietveld method (Rietveld 1969).

Carbon and oxygen isotope analyses of six bulk layer subsamples from FTOP were determined at the Stable Isotope Analysis Service of the University of Salamanca (Spain). Extraction of CO₂ for isotopic analyses followed standard techniques (McCrea 1950) using an ISOCARB device connected to a SIRA series 10 mass spectrometer from VG Iso-tech. The isotope analysis of the other travertine samples (FTNP) was performed at the Laboratory of Biogeochemistry of Stable Isotopes of the Andalusian Institute of Earth Sciences (CSIC) of Granada (Spain). The methodology for CO₂ extraction was the same, but the analyses were done using the GasBench II connected to the Finnigan DeltaPLUS XP isotope ratio mass spectrometer (IRMS). Overall analytical precision, as standard deviation ($N=12$), is better than ± 0.08 ‰ for $\delta^{13}\text{C}$ and ± 0.17 for $\delta^{18}\text{O}$ values of carbonates. Accuracy is routinely checked by replicate measurements of laboratory standards and it is better than ± 0.12 ‰. Results are reported in the familiar $\delta\text{‰}$ notation relative to V-PDB and V-SMOW.

Applications of the stable isotope fractionation

The use of the stable isotope fractionation equations for paleoclimatic and paleoenvironmental reconstructions is based on the fact that the isotope fractionation between a mineral phase and the water, from which it is precipitating, is a function of the temperature as long as the precipitation takes place in thermodynamic equilibrium (e.g., Zheng 1999, 2011 and references therein), and therefore, the isotopic values of the solids represent the water temperature at the moment of precipitation (e.g. Fouke et al. 2000; Zhou and Zheng 2003; Pentecost 2005; Liu et al. 2006; Kele et al. 2008, 2011, 2015; Pedley 2009; Gabitov 2013; Osácar et al. 2013, 2016; Capezzuoli et al. 2014; Lachniet 2015).

In the case of the $\delta^{13}\text{C}$ isotope data, this paleotemperature indication can only be obtained using the $\delta^{13}\text{C}$ fractionation between calcite–aragonite and the dissolved CO₂, since this fractionation is temperature-dependent (e.g., Romanek et al. 1992; Scheele and Hoefs 1992; Chacko et al. 2001). The problem in the present study is that the $\delta^{13}\text{C}$ value in CO₂ is not available in the analysed waters; instead, the $\delta^{13}\text{C}$ value was measured in the dissolved inorganic carbon (DIC), which, in these waters, could be assumed to mostly be as HCO₃⁻ (see below). The $\delta^{13}\text{C}$ fractionation between the carbonate solids (calcite or aragonite) and the HCO₃⁻ is independent of the temperature (Rubinson and Clayton 1969; Turner 1982; Romanek et al. 1992) and for the range between 10 and 40 °C, the reported values are $2.7 \pm 0.6\text{‰}$ for aragonite–HCO₃⁻ fractionation and $1 \pm 0.2\text{‰}$ for calcite–HCO₃⁻ fractionation. In summary, the measured $\delta^{13}\text{C}$ cannot be used to make a temperature estimation in the

Fitero system, but it can help to evaluate the $\delta^{13}\text{C}$ fractionation during the travertine precipitation, which is what will be shown in section “ $\delta^{13}\text{C}$ ”.

There is much more information about the $\delta^{18}\text{O}$ fractionation and its study has been quite thorough. Several fractionation equations, based on inorganic and biogenic carbonates, have been proposed for the $\delta^{18}\text{O}$ equilibria between aragonite and water and between calcite and water and the more suitable were selected according to the identified mineralogy of the travertines under study. The FTOP travertines are almost pure aragonite and the equations used in this work were the ones listed next, including those for biogenic aragonite to check their applicability to inorganic aragonite travertines (Table 1):

- Grossman and Ku (1986): equation deduced from aragonite foraminifera, gastropods, and scaphods in the range of 2.5–26 °C.
- Patterson et al. (1993): derived from the study of aragonite fish otoliths in the range of 3.2–30.3 °C.
- Thorrold et al. (1997): also derived from aragonite fish otoliths but in the temperature range of 18–25 °C.
- White et al. (1999): deduced from marine molluscs in the range of temperatures from 8 to 24 °C.
- Böhm et al. (2000): derived from aragonite sponges in the temperature range of 3–28 °C.
- Zhou and Zeng (2003): derived from experiments of aragonite precipitation in the temperature range of 10–70 °C.
- Kim et al. (2007): derived from experiments with inorganic synthetic aragonites in the temperature range of 10–40 °C. This equation has been corrected for the conventional CO₂–aragonite acid fractionation factor and the equation in Lachniet (2015) has been used.
- Chacko and Deines (2008) calculated the partition function ratios (for aragonite and water) from statistical mechanical calculation and a compilation of vibrational frequency data. The equation is applicable at temperatures between 0 and 130 °C.
- Wang et al. (2013): equation derived from aragonite precipitation from seawater experiments in the temperature range of 25–55 °C.
- Kele et al. (2015): equation proposed from a set of samples constituted by mixtures of calcite and aragonite travertines precipitated between 20 and 95 °C (they also proposed another equation including tufas, not shown here, with very similar results).

The FTNP sample consists of a mixture of aragonite and calcite, and for the $\delta^{18}\text{O}$ fractionation evaluation, three equations have been used: the just mentioned equation proposed by Kele et al. (2015) as it corresponds to a mixture

Table 1 Aragonite–water, calcite–water, and calcite + aragonite–water fractionation equations used in this study

	Author	Fractionation equation
$\delta^{18}\text{O}_{\text{aragonite-water}}$	Grossman and Ku (1986)	$1000 \ln \alpha = 18.04 \times \frac{1000}{T} - 31.12$
	Patterson et al. (1993)	$1000 \ln \alpha = 18.56 \times \frac{1000}{T} - 33.49$
	Thorrold et al. (1997)	$1000 \ln \alpha = 18.56 \times \frac{1000}{T} - 32.54$
	White et al. (1999)	$1000 \ln \alpha = 16.74 \times \frac{1000}{T} - 26.39$
	Böhm et al. (2000)	$1000 \ln \alpha = 18.45 \times \frac{1000}{T} - 32.54a$
	Zhou and Zheng (2003)	$1000 \ln \alpha = 20.44 \times \frac{1000}{T} - 41.48$
	Kim et al. (2007)	$1000 \ln \alpha = 17.88 \times \frac{1000}{T} - 30.76$
	Chacko and Deines (2008) ^a	$1000 \ln \alpha = -12.815 + 5.793x - 3.7554 \times 10^{-1}x^2$ $+ 3.2966 \times 10^{-2}x^3 - 2.2189 \times 10^{-3}x^4 + 8.9981$ $\times 10^{-5}x^5 - 1.636 \times 10^{-6}x^6$
	Wang et al. (2013)	$1000 \ln \alpha = 22.5 \times \frac{1000}{T} - 46.1$
$\delta^{18}\text{O}_{\text{calcite+aragonite-water}}$	Kele et al. (2015)	$1000 \ln \alpha = 20 \times \frac{1000}{T} - 36$
$\delta^{18}\text{O}_{\text{calcite-water}}$	Kim and O'Neil (1997)	$1000 \ln \alpha = 18.03 \times \frac{1000}{T} - 32.17$
	Coplen (2007)	$1000 \ln \alpha = 17.4 \times \frac{1000}{T} - 28.6$

Temperature (T) is in Kelvin. α is the fractionation between carbonate and water calculated as $(1000 + \delta^{18}\text{O}_{\text{aragonite}})/(1000 + \delta^{18}\text{O}_{\text{water}})$ or $(1000 + \delta^{13}\text{C}_{\text{aragonite}})/(1000 + \delta^{13}\text{C}_{\text{water}})$ being $\delta^{18}\text{O}$ values vs. V-SMOW and $\delta^{13}\text{C}$ values vs. V-PDB

^a $x = 10^6/T^2$, where T is Kelvin

of aragonite and calcite, and two of the most used calcite equilibrium equations (Kim and O'Neil 1997; Coplen 2007) which cover almost the whole range of values given by the rest of the calcite–water fractionation equations presently available:

- Kim and O'Neil (1997) derived the equation from inorganic calcites synthesised in laboratory in the range of 10–40 °C. It has been corrected for the conventional CO_2 –calcite acid fractionation factor of 1.01025 (Friedman and O'Neil 1977) and
- Coplen (2007) proposed the equation from vein calcite samples from Devils Hole (Nevada, USA).

Results

Main characteristics of the thermal waters

Only the most relevant information of the Fitero thermal waters for the present study will be highlighted here. A thorough study of their chemical characteristics (and some modelling results) can be found in another paper from Blasco et al. (2019). Table 2 shows the chemical and isotopic data of the thermal water taken in the main spring (F1) and the analytical data of the water sample taken in the new pipe (FWNP; Fig. 3a). The temperature of the thermal water (F1) is 45.5 °C and its pH is near neutral. The water in the new pipe was at 33 °C in the moment of sampling and the pH was

Table 2 Chemical and isotopic analyses of the Fitero thermal water that springs in the Becquer spa (F1; whose chemical composition is constant over time) and the chemical analysis of a water sample taken at the exit of a discharging pipe from the spa (FWNP)

	F1	FWNP
Temperature (°C)	45.50	33
TDS	4820.2	4423
pH	6.86	7.72
HCO_3^-	174.02	125
Cl^-	1610	1505
SO_4^-	1376	1290
Ca	469	441
Mg	92.10	80.8
Na	981	920
K	30.20	30.3
Sr	11.10	10.3
SiO_2	23.75	
Fe	0.13	
$\delta^{18}\text{O}$ in H_2O (V-SMOW)	−8.7	
$\delta^2\text{H}$ in H_2O (V-SMOW)	−63.9	
$\delta^{13}\text{C}$ in DIC (V-PDB)	−8.42	

TDS (calculated using PHREEQC) and dissolved elements are expressed in ppm

higher than in F1. As mentioned before, it was impossible to get a water sample from the old pipe, but considering its location, their chemical characteristics would be very similar to the main spring (F1) except for a temperature of 40 °C.

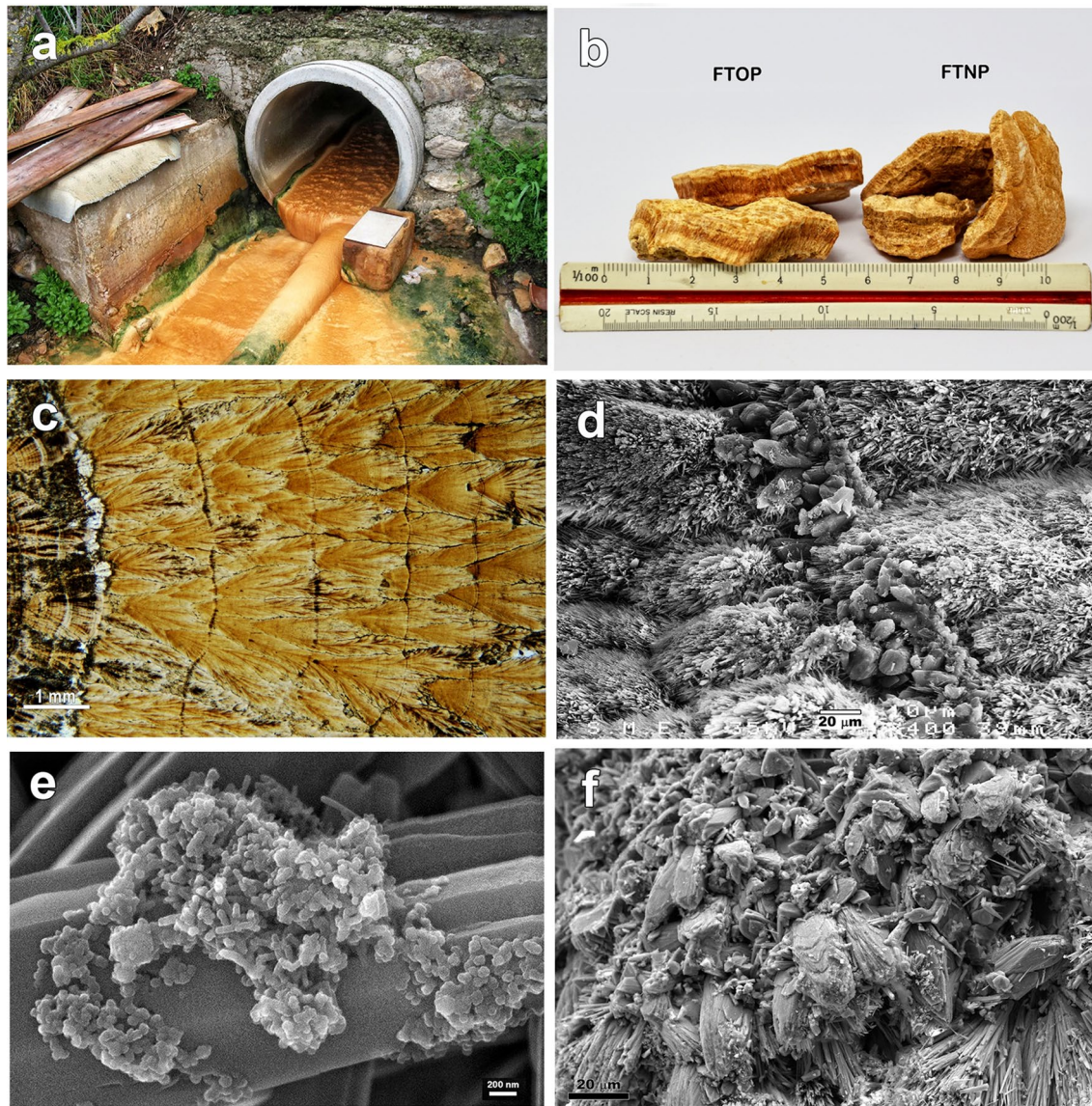


Fig. 3 **a** New pipe at its discharge point on the Cidacos river, where travertine FTNP is precipitating. **b** FTOP and FTNP travertine samples where the alternation between yellowish and reddish bands can be seen. **c** Photograph taken with a petrographic microscope showing the fibrous-radial texture with fan-shaped aggregates (FTOP). **d** FESEM image of the FTOP travertine showing the aragonitic bands

(on the right and left of the image) and a calcite interlayer in between. Some disperse calcite crystals in the aragonite can also be appreciated. **e** FESEM image of the FTOP travertine with a detail of an aragonite needle with iron oxy-hydroxides growing on it. **f** FESEM image of the FTNP travertine where abundant calcite crystals can be identified, while aragonite needles are less common

The $\delta^{18}\text{O}$ and $\delta^2\text{H}$ values in F1 (-8.7 and -63.9 ‰, respectively; Table 2) suggest a meteoric origin of the thermal water, since they are close to the Global Meteoric Water Line ($\delta^2\text{H}=8\delta^{18}\text{O}+10$; Craig 1961) and the Spanish Meteoric Water Line calculated from the data of the Spanish Network for the control of the isotopes in the rainfall ($\delta^2\text{H}=8\delta^{18}\text{O}+9.27$; Díaz-Teijeiro et al. 2009). The $\delta^{13}\text{C}$ value in the dissolved inorganic carbon of the thermal water is -8.4 ‰ (Table 2) and it suggests that, after infiltration through the soils (degradation of C3-type plants results in $\delta^{13}\text{C}$ values of about -23 ‰; Clark and Fritz 1997), the thermal water

interacts with carbonate rocks in the aquifer (with $\delta^{13}\text{C}$ values around 0 ‰; Clark and Fritz 1997; Fig. 4).

Some speciation-solubility calculations were carried out with the geochemical code PHREEQC (Parkhurst and Appelo 2013) and the WATEQ4F thermodynamic database. The main results related to the carbonate system show that calcite and aragonite are in equilibrium or close to equilibrium at spring temperature in F1 (saturation states of 0.14 and 0.01, respectively) and with a high $\log p\text{CO}_2$, -1.58 , whilst these minerals are more oversaturated (0.7 and 0.54, respectively) in the water sample FWNP due to an important

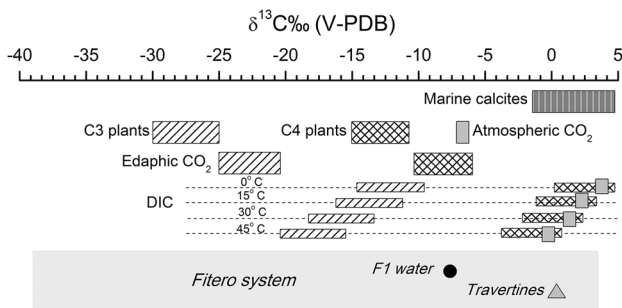


Fig. 4 $\delta^{13}\text{C}$ composition of the Fitero thermal water and the travertine precipitated from it (the travertine representation include all the bands of FTOP sample and the FNTP sample, since the values are between 0.9 and 0.3‰). The isotopic values of the possible $\delta^{13}\text{C}$ sources are shown in the upper part of the graph. The equations described by Romanek et al. (1992) have been used for the calculation of the isotopic theoretical signature of DIC. Figure modified from Delgado and Reyes (2004) and Reyes et al. (1998)

CO_2 outgassing during the circulation of the waters through the pipe giving a $\log p\text{CO}_2$ of -2.7 and justifying a pH value higher than in F1. The amount of CO_2 outgassing and calcium carbonate precipitation can be calculated by a simple mass balance between the two waters and the results indicate that there are 0.614 mmol/L of CO_2 loss which leads to the precipitation of 0.71 mmol/L of calcium carbonate. Therefore, calcium carbonate was precipitating in the moment of the water sampling in the new pipe, indicating that the CO_2 outgassing is the triggering factor of the carbonate precipitation, promoted by the high $p\text{CO}_2$ and the high temperature of the waters at the spring (CO_2 solubility is lower at higher temperatures, facilitating the degassing to the atmosphere).

This outgassing process must have also taken place in the water circulating through the old pipe to promote the precipitation of the aragonite travertine. The source water was the same thermal spring F1, whose compositional characteristics show minor variations with time (e.g., Auqué et al. 1989; Blasco et al. 2019). Therefore, similar equilibrium conditions with respect to calcite and/or aragonite should prevail at the moment of emergence and CO_2 degassing would be necessary to trigger the precipitation of carbonates (otherwise, as the solubility of these minerals increase with the decrease of temperature, the waters, initially in equilibrium in the spring, would have suffered the opposite effect in the cooling pool, the undersaturation with respect to the carbonates).

Main characteristics of the travertines

The travertine samples consist of an alternation of yellowish and reddish bands (Fig. 3b). Each band is also constituted by a thin lamination barely distinguishable at a glance but evident when studying the thin sections under

the petrographic microscope. This lamination is not related to temporal (or climatic) variations but to the intermittent discharge through the pipes and, therefore, they are conditioned by the availability of water, as also described by Rodríguez-Berriguete et al. (2018) in other human-induced travertines.

Although both travertines look similar, their mineralogy is quite different. The XRD analyses of two yellowish and two reddish bands of sample FTOP indicate a proportion of aragonite higher than 98% with minor amounts of calcite, and this is common to both types of bands. The mineralogical results for sample FTNP (from the new pipe; Fig. 3a) indicate a higher proportion of calcite (about 60%) and much less aragonite (40%), as an average from one yellowish and one reddish band.

The detailed mineralogical examination of FTOP allowed identifying additional relevant characteristics of the aragonite travertines: (1) the petrographic microscope showed a fibrous-radial, fan-shaped texture in the aragonite (Fig. 3c) which, in the FESEM, is seen as elongated prisms or needles aggregated forming bushes (Fig. 3d); (2) the presence of disperse calcite in all bands is mainly associated with the thin inter-layers between yellowish and reddish aragonite bands, whilst there is not a preferential distribution of calcite or aragonite in the FTNP travertine (Fig. 3d, f); (3) lump aggregates of amorphous oxy-hydroxides have been identified on the aragonite needles in the reddish bands (Fig. 3e) and they, probably, are responsible for the colour of the bands despite their low content (unidentified by XRD and coherent with the low dissolved Fe in waters; Table 2).

Examination of thin sections and detailed FESEM observations show no evidence of microbial activity (e.g., biofilms or extracellular polymeric substances, EPS) in the travertines. These evidences are not usually preserved in old travertines (Jones and Renaut 1995; Peng and Jones 2012), but given that the samples studied here are from an active deposit, the lack of them suggests an abiogenic origin (Jones 2017a).

Additionally, the possibility of widely known transformation aragonite–calcite has been discarded, since calcite and aragonite layers are separated by well-defined limits (Jones and Peng 2014), and moreover, calcite does not show any aragonite relict or dissolution signs (Wassenburg et al. 2016).

Isotopic determinations of $\delta^{18}\text{O}$ and $\delta^{13}\text{C}$ in the carbonates were made in the travertine sample FTNP (whole sample) and in six subsamples of FTOP, in three reddish bands (FTOP-R1, R2, R3), and in three yellowish bands (FTOP-Y1, Y2, Y3; Table 3). The results show that the $\delta^{18}\text{O}$ values are similar in all the bands of the aragonite travertine and also in the calcite–aragonite travertine between 17.72 and 17.93‰ vs. V-SMOW. With respect to the $\delta^{13}\text{C}$ values (‰ vs. V-PDB), they are higher in the yellowish

Table 3 Isotopic data of travertine samples: the reddish bands (FTOP-R) and the yellowish bands (FTOP-Y) of sample FTOP, and the whole sample of travertine FTNP

	$\delta^{13}\text{C}$ (V-PDB)	$\delta^{18}\text{O}$ (V-PDB)	$\delta^{18}\text{O}$ (V-SMOW)
FTOP-R1	0.54	−12.62	17.90
FTOP-R2	0.54	−12.79	17.72
FTOP-R3	0.37	−12.75	17.76
FTOP-Y1	0.86	−12.39	17.93
FTOP-Y2	0.80	−12.68	17.83
FTOP-Y3	0.79	−12.73	17.79
FTNP	0.87	−12.61	17.85

bands (FTOP-C) and in sample FTNP, with values around 0.8‰, than in the reddish bands, between 0.37 and 0.54‰ (Table 3).

Discussion

There are two main issues to be discussed here. The first one refers to the different mineralogical composition of the two studied travertine samples (different amounts of aragonite and calcite) and the second refers to their isotopic composition and their possible use as paleoenvironmental indicators.

Mineralogy

There are several classical studies on the main factors controlling calcite or aragonite precipitation in natural geological samples and in laboratory experiments (Folk 1994; Fouke et al. 2000; Pentecost 2005; Jones 2017b; and references therein). These factors are: temperature, Mg/Ca ratio in the water, dissolved strontium content, CO₂ content and degassing, and the biological influence. Except for the last factor, that will not be discussed here, since no evidence of biological effects have been found in the studied travertines, an evaluation of the influence of the other controlling factors is presented next.

Temperature and magnesium concentration have been considered the most important factors controlling the mineralogy of the precipitated carbonates. Generally speaking, aragonite is considered to precipitate at higher temperatures than calcite; for example, Folk (1994) observed that aragonite precipitates if the temperature is higher than 40 °C irrespective of the water composition, and calcite would precipitate if the temperature of the water is lower than 40 °C and it is Ca-rich. Fouke et al. (2000), in the same line, indicated that if the temperature is higher than 44 °C only aragonite precipitates, if the temperature is lower than 30 °C only calcite does, and when it is between 30 and 43 °C, both mineral phases precipitate together. However, aragonite is not always

favoured over calcite at this “critical temperature” of about 40 °C; for example, calcite has been found to precipitate in Egerszalók (Hungary) at a temperature of about 70 °C (Kele et al. 2008) and in North Island (New Zealand), where the water temperature is higher than 90 °C (Jones et al. 1996; see also the review by Jones 2017b).

Regarding the magnesium concentration in the waters, Fischbeck and Müller (1971) stated that aragonite precipitation is significant if the Mg/Ca ratio is higher than 2.9; Folk (1994) reported that aragonite would precipitate if the Mg/Ca ratio of the water is higher than 1:1 no matter the water temperature; and AlKhatib and Eisenhauer (2017) indicated that any Mg/Ca ratio higher than 2:1 will assure aragonite precipitation even at temperatures of only 12.5 °C. Furthermore, in some lakes in the Great Plains of North America, the evaporation produces high Mg/Ca ratios that trigger the precipitation of aragonite despite a temperature of the water lower than 30 °C (Last 1989; Last et al. 1998).

In the case of sample FTOP, the temperature of the parental water is 40 °C and the composition is assumed to be the same as the thermal water F1, with a very low Mg/Ca ratio of 0.32. According to the previous authors, the water temperature would favour aragonite precipitation, despite the low Mg/Ca ratio which would allow the precipitation of some minor amounts of calcite. This is exactly what has been observed and, therefore, the thin calcite inter-layers between the aragonite bands seem to represent inter-discharge periods when the remaining water would probably have a temperature lower than 40 °C. In the case of sample FTNP, the Mg/Ca ratio in the parental water (FWNP) is 0.27, very similar to the F1 sample, but the temperature of the water discharged through the pipe varies between 40 and 33 °C which would explain the higher proportion of calcite. Therefore, in these travertines, temperature seems to be the main control of the mineralogy.

Other controlling factors may play a role, additionally to, or interplayed with, temperature (Jones, 2017b). Some authors argue that the Sr content in the waters favours aragonite precipitation and inhibits calcite growth, but others state that the higher Sr concentrations in aragonite, in comparison to calcite, are only due to the partition coefficients, which are higher in aragonite (Sr incorporates easier in aragonite lattice than in calcite). The fact that the two travertine samples FTOP and FTNP have precipitated from a very similar water with similar Sr content (Table 2) and one of them is almost pure aragonite and the other has 60% of calcite supports the hypothesis that the dissolved content of Sr is not an important controlling factor of the mineralogical phase, at least in our system.

Finally, regarding the importance of CO₂ content and outgassing rate, some authors reported that aragonite precipitation is favoured by high CO₂ contents and degassing rates as it is common in thermal springs (Kitano 1963; Chafetz

Table 4 Fractionation equations for the $\delta^{13}\text{C}$ in CO_2 estimation from $\delta^{13}\text{C}$ in the carbonate or $\delta^{13}\text{C}$ in HCO_3 dissolved

	Author	Equation
$\text{CaCO}_3\text{--CO}_2$	Panichi and Tongiorgi (1976)	$\delta^{13}\text{C}_{\text{CO}_2} = 1.2(\delta^{13}\text{C}_{\text{CaCO}_3}) - 10.5$
	Romanek et al. (1992) ^a	$10^3 \ln \alpha^{13}\text{C}_{\text{aragonite--CO}_2} = 13.88 - 0.137T$
	Romanek et al. (1992) ^a	$10^3 \ln \alpha^{13}\text{C}_{\text{calcite--CO}_2} = 11.98 - 0.127T$
$\text{HCO}_3\text{--CO}_2$	Mook et al. (1974) ^b	$10^3 \ln \alpha^{13}\text{C}_{\text{HCO}_3\text{--CO}_2} = 9.522(10^3 T^{-1}) - 24.1$
	Zhang et al. (1995) ^a	$10^3 \ln \alpha^{13}\text{C}_{\text{HCO}_3\text{--CO}_2} = -0.0954T + 10.41$
	Szaran (1997) ^a	$10^3 \ln \alpha^{13}\text{C}_{\text{HCO}_3\text{--CO}_2} = -0.1141T + 10.78$

^aTemperature (T) is in $^\circ\text{C}$ ^bTemperature (T) is in Kelvin

et al. 1991; Jones 2017b). As stated above, CO_2 outgassing is the triggering factor of carbonate precipitation in the studied travertines, since the spring waters are in equilibrium, or near equilibrium, with respect to aragonite and calcite. However, differences in the rate of CO_2 outgassing may also promote variations in the oversaturation degree and, in turn, in the precipitated carbonate phase (Jones and Peng 2016; Jones 2017b). The travertines studied here precipitate inside inclined pipes where an important outgassing rate is expected. However, differences may arise by variations in the discharge and/or in the distance of the precipitates from the spring.

In the case of the pure aragonite travertine FTOP, precipitated from waters at nearly constant temperatures ($40\text{ }^\circ\text{C}$), the possible variations in the outgassing rate do not seem to induce important mineralogical changes. Only the thin calcite inter-layers between the aragonite bands, which, as mentioned above, is interpreted as representing inter-discharge periods, could be related to water temperatures lower than $40\text{ }^\circ\text{C}$ or to periods of lower discharge and lower CO_2 outgassing rate.

The FTNP travertine, located farther away from the thermal waters source than the FTOP deposits, is associated with a wider range of water temperatures ($33\text{--}40\text{ }^\circ\text{C}$) and with more variable discharge regimes. In the moment of the sampling of FWNP, the water temperature was $33\text{ }^\circ\text{C}$ (Table 2) and the discharge was low. Higher discharges, higher water temperatures, and, most probably, also higher CO_2 outgassing rates, occur in this pipe during the spa activity. Therefore, coupled changes in temperature and CO_2 outgassing rates may also be the cause of the higher proportions of calcite in this deposit, although more detailed studies would be necessary to clarify this hypothesis.

Stable isotopes

$\delta^{13}\text{C}$

The $\delta^{13}\text{C}$ values of travertines are considered to reflect the origin of the CO_2 in the source water in the classification scheme of Pentecost (2005) which includes two main

travertine types, thermogene and meteogene. Thermogene travertines are those in which the CO_2 has a deep origin (magmatic or from decarbonation processes) and $\delta^{13}\text{C}$ values range from -1 to $+10\text{‰}$. Travertines are considered as meteogene if the CO_2 has a shallow origin, mainly meteoric, and they can be divided in ambient and superambient (or thermometeogene). The ambient meteogene travertines are formed at ambient temperatures (waters have not suffered a heating process) and they display $\delta^{13}\text{C}$ values ranging from -12 to -3‰ . The superambient meteogene travertines precipitate from warm waters (waters heated through deep circulation and emerging as hot springs) and have $\delta^{13}\text{C}$ values ranging from -12 to $+2\text{‰}$. The $\delta^{13}\text{C}$ data in the studied travertines range from 0.37 to 0.87‰ (Table 3) and, therefore, they could be classified as superambient meteogene or thermometeogene travertines.

However, the source of CO_2 can only be properly assessed from the $\delta^{13}\text{C}$ values in travertines where secondary modifications (e.g. CO_2 outgassing) of the isotopic carrier are minimised (e.g., close to the spring orifice; Kele et al. 2011; Jones and Peng 2016 and references therein) and this is not exactly the case here. Fitero travertines have precipitated after CO_2 degassing of the thermal waters (see above) and, therefore, their $\delta^{13}\text{C}$ values would reflect the $\delta^{13}\text{C}$ in the dissolved CO_2 at the moment of travertine precipitation. To better check the meaning of the values analysed in the travertines, the $\delta^{13}\text{C}$ in the CO_2 at the precipitation moment and, in the spring conditions, previous to the CO_2 outgassing, have been calculated.

As previously done by other authors (e.g., Minissale 2004; Kele et al. 2008, 2011; Sierralta et al. 2010; Jones and Peng 2016), the $\delta^{13}\text{C}$ in the travertine can be used to estimate the $\delta^{13}\text{C}$ in the dissolved CO_2 at the moment of travertine precipitation, using the equation proposed by Panichi and Tongiorgi (1976; Table 4). Applying this equation to the travertine samples studied here (aragonite and calcite–aragonite), the $\delta^{13}\text{C}_{\text{CO}_2}$ obtained range from -10 to -9.5‰ . However, since this equation does not take into account the $\delta^{13}\text{C}$ dependence on temperature, the calculations were repeated with the equations proposed by Romanek et al.

(1992; Table 4) for the $\delta^{13}\text{C}$ fractionation between aragonite (or calcite) and CO_2 .

The $\delta^{13}\text{C}_{\text{CO}_2}$ values obtained for the FTOP samples (aragonite), assuming a precipitation temperature of 40 °C, were from -8.3 to -7.8‰ . For sample FTNP, the precipitation temperatures considered for the calculation were between 33 and 40 °C (possible range of the circulating waters) and the values obtained were between -7.2 and -6.3‰ . In summary, considering all the results obtained with the equations proposed by Romanek et al. (1992), the $\delta^{13}\text{C}$ in the dissolved CO_2 when the travertine precipitated was in the range of -8.3 to -6.3‰ .

These values were then compared with the $\delta^{13}\text{C}$ in the CO_2 calculated in the emergence spring (water sample F1). This last value was theoretically approximated from the $\delta^{13}\text{C}$ analysed in the DIC (dissolved inorganic carbon), assuming that the DIC mainly corresponds to HCO_3^- (the pH value of the spring water is near 7; Table 2) and using the equations proposed by Mook et al. (1974), Zhang et al. (1995) and Szaran (1997) for the $\delta^{13}\text{C}$ fractionation between HCO_3^- and CO_2 (Table 4). A good agreement around -15‰ was obtained among all these equations.

Two main conclusions can be extracted from these results:

- First, the $\delta^{13}\text{C}$ value calculated for the CO_2 at spring conditions, and the hydrogeological and hydrogeochemical characteristics of the Fitero geothermal system (Blasco et al. 2019), support the classification of the travertines as thermometeogene, derived from waters heated by a deep circulation but without an “endogenous” $\delta^{13}\text{C}$ component (Pentecost 2005). In this scheme, carbon dissolved from the carbonate rocks in the aquifer (with $\delta^{13}\text{C}$ values usually between -1 and 5‰ ; Fig. 4) would influence the $\delta^{13}\text{C}$ values of the waters (and travertines) shifting them towards isotopically heavier values than those in the recharge waters (Fig. 4).
- Second, the $\delta^{13}\text{C}$ values calculated for the CO_2 at spring condition (-15‰) are more negative than at the moment of the travertine precipitation (-8.3 to -6.3‰). These numbers would be consistent with the aforementioned existence of a CO_2 outgassing process (resulting in the $\delta^{13}\text{C}$ enrichment in the CO_2 of the waters) as the trigger of travertine precipitation.

$\delta^{18}\text{O}$

As mentioned above, although with some uncertainties related to the possible equilibrium situations between the solids and their parental waters, the use of $\delta^{18}\text{O}$ in aragonite (or calcite) for paleoclimatic and paleoenvironmental reconstructions is a very useful tool. There are some examples in natural systems of travertine precipitation under, or close to, equilibrium conditions with respect to some of the

fractionation equations (Chafetz et al. 1991; Garnett et al. 2004; Coplen 2007; Li et al. 2011, 2012; Yan et al. 2012; Lachniet et al. 2012; Osácar et al. 2016, 2013; Wang et al. 2014; Kele et al. 2015; Asta et al. 2017; Arenas et al. 2018). However, there are also examples where equilibrium is not maintained during precipitation (Friedman 1970; Fouke et al. 2000; Lojen et al. 2004, 2009; Coplen 2007; Kele et al. 2008, 2011; 2015; Demény et al. 2010; Yan et al. 2012; Wang et al. 2014; Asta et al. 2017; Zavidlav et al. 2017).

The study of an active precipitation system, like the one presented here, provides the possibility to compare the temperature results obtained from the application of the $\delta^{18}\text{O}$ “equilibrium” fractionation equations and the temperature actually measured in the parental water. This will give a better knowledge of the processes affecting the isotopic equilibrium and will help to interpret the isotopic signature of old travertines.

To do that, several equations (section “Applications of the stable isotopes fractionation”) have been applied for $\delta^{18}\text{O}$ equilibrium between the aragonites from sample FTOP (the six subsamples) and the equivalent to their parental water, F1 with 40 °C. For comparative purposes, some of the aragonite and calcite equilibrium equations (section “Applications of the stable isotopes fractionation”) have been used for the sample FTNP (constituted by a mixture of calcite and aragonite) and the water F1 (at 40 °C), because, unfortunately, there is not isotopic information from its own parental water FWNP.

All fractionation equations used here have been represented in Fig. 5. Panel a shows the equations for aragonite and panel b shows the equations for calcite (or for a mixture of calcite and aragonite). The isotopic values of the studied travertines at their precipitation temperatures are also shown: six open circles for the aragonite travertine in Fig. 5a, and a grey rectangle representing the calcite–aragonite travertine and the interval between 33 and 40 °C that covers the temperature variation of the water circulating through the pipe, in Fig. 5a, b. As it can be seen, all the travertine samples fall in the “equilibrium window” defined by the area covered by all the fractionation equations, suggesting that they have precipitated under, or close to, isotope equilibrium (e.g. Lachniet 2015). However, this overall “equilibrium” situation is translated to a relatively wide range of possible temperatures covered by the whole set of considered equations (Table 5).

Regarding the pure aragonite travertine FTOP, there are two equations that provide discrepant temperatures (Table 5): (1) the one proposed by Zhou and Zheng (2003) which gives a temperature about 30 °C (probably due to the existing controversy about the experimental conditions for its determination; Kim and O’Neil 2005; Horita and Clayton 2007; Lécuyer et al. 2012; Wang et al. 2013) and (2) the empirical equation from Kele et al. (2015), which provides a temperature of almost 48 °C, which is higher

Fig. 5 **a** Representation of the $\delta^{18}\text{O}$ aragonite–water equilibrium lines proposed by different authors and considered in this study. **b** The two most used equations for calcite: Kim and O’Neil (1997) and Coplen (2007); the equation from Kele et al. (2015) is also included, since it was calculated using a mixture of calcites and aragonites. The samples from travertine FTOP (98% aragonite) are shown as open circles in **a** and the travertine FTNP (60% calcite) is represented over the possible range of precipitation temperatures (33–40 °C) in **a** and **b**

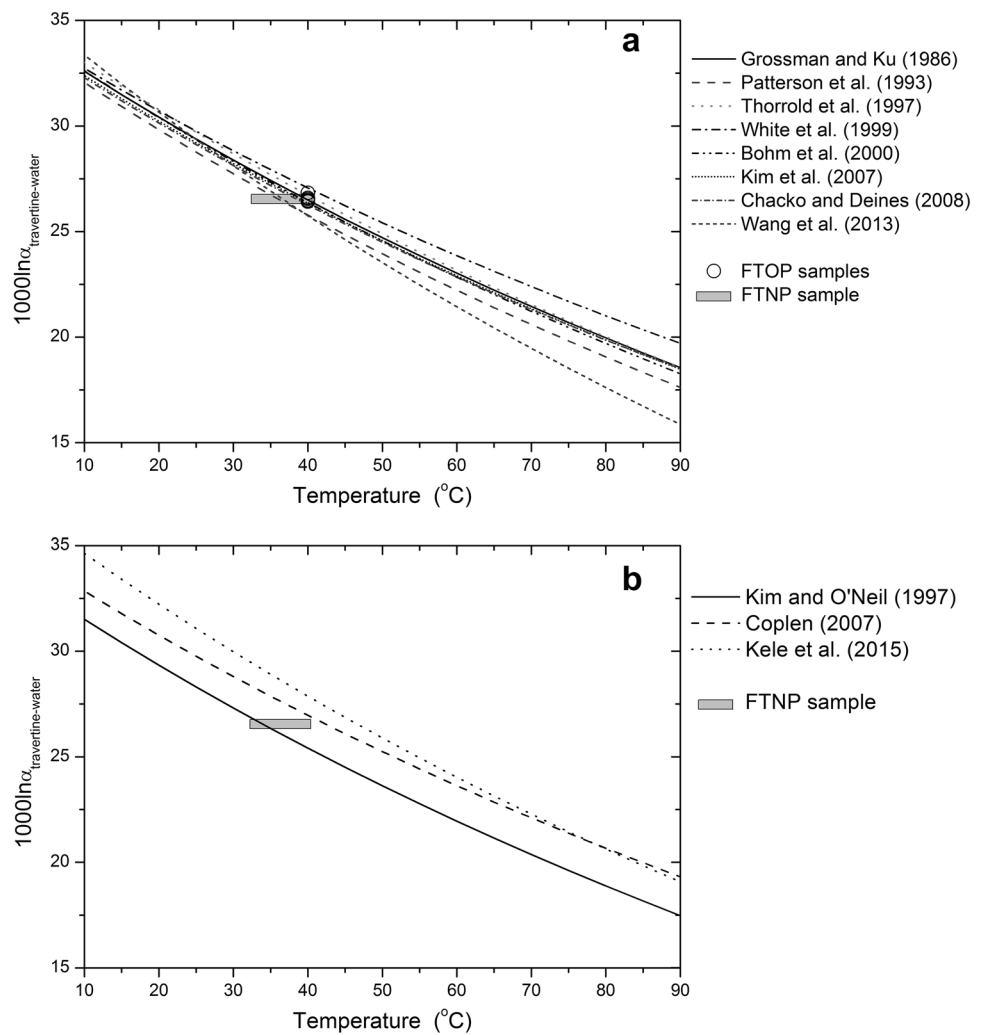


Table 5 Temperatures (°C) obtained with different oxygen isotope aragonite–water equilibrium equations

		FTOP-R1	FTOP-R2	FTOP-R3	FTOP-Y1	FTOP-Y2	FTOP-Y3	FTNP
$\delta^{18}\text{O}_{\text{aragonite-water}}$	Grossman and Ku (1986)	40.1	41.0	40.8	39.9	40.4	40.7	40.3
	Patterson et al. (1993)	36.4	37.3	37.0	36.2	36.7	37.0	36.3
	Thorrold et al. (1997)	41.3	42.3	42.1	41.2	41.7	42.0	41.3
	White et al. (1999)	43.5	44.5	44.3	43.3	43.9	44.2	43.5
	Böhm et al. (2000)	39.5	40.4	40.2	39.3	39.8	40.1	39.7
	Zhou and Zheng (2003)	27.6	28.4	28.2	27.5	27.9	28.1	27.6
	Kim et al. (2007)	39.2	40.2	40.0	39.1	39.6	39.9	39.5
	Chacko and Deines (2008)	38.8	39.7	39.5	38.6	39.1	39.4	38.4
	Wang et al. (2013)	36.9	37.6	37.4	36.7	37.1	37.4	37.0
$\delta^{18}\text{O}_{\text{calcite+aragonite-water}}$	Kele et al. (2015)	47.0	47.9	47.7	46.8	47.3	47.6	46.9
	$\delta^{18}\text{O}_{\text{calcite-water}}$							
	Kim and O’Neil (1997)	–	–	–	–	–	–	43
	Coplen (2007)	–	–	–	–	–	–	34.5

The water isotope values used for these calculations are in all the cases those of water sample F1

than the possible parental water (probably due to the fact that the fitting of this equation was strongly influenced by five samples with very high fractionation of unclear origin; Kele et al. 2015). In both cases, the results should be used with caution and they would not be taken into account in the discussion below. The temperature obtained using the rest of the equations, regardless if they were calibrated using biogenic or inorganic aragonites, is about 40 °C, which is the temperature at which the precipitation actually takes place. These coincident results could be expected as the equations used here are within the uncertainty range defined by Kim et al. (2007) in their calibration ($\pm 0.46\%$, see Fig. 5 in Kim et al. 2007).

The results obtained for the travertine FTNP merit some additional considerations, in terms of comparison with FTOP, as it is constituted by a mixture of calcite (about 60%) and aragonite (40%), and the specific mineralogy could be an important factor when studying the $\delta^{18}\text{O}$ isotope signature of carbonates.

The relative fractionation factor between calcite and aragonite is still under debate: some authors have experimentally found that the oxygen isotope fractionation is lower between aragonite and water than between calcite and water, whereas others have found the opposite (e.g., Kele et al. 2008; Lécuyer et al. 2012; Wang et al. 2013; and references therein). In the case studied here, a relation between the values and the percentages of calcite or aragonite is not observed as the $\delta^{18}\text{O}$ values are similar in the FTOP and FTNP travertines. Therefore, no differences between the calcite–water and aragonite–water oxygen fractionation are evident, as it has also been observed in other travertines constituted by calcite and aragonite (e.g., Jones and Peng 2014; Kele et al. 2015).

In the cases like FTNP, it is impossible to evaluate the $\delta^{18}\text{O}$ fractionation in each mineral phase, intermixed at microscale, in a separate way (e.g., Jones and Peng 2014, 2016) and some authors have suggested to use aragonite and calcite calibration equations over the same sample, as if it was pure aragonite or pure calcite, to estimate temperatures/paleotemperatures (e.g., Jones and Peng, 2016).

When the aragonite equations are used for the fractionation of the travertine FTNP and the thermal water F1, the temperature obtained is about 40 °C, which is close to the maximum real temperature in this pipe. It is also the same as the temperature calculated for the aragonite travertine FTOP in the six subsamples (Table 5), which is reasonable, since the $\delta^{18}\text{O}$ value is very similar in all the travertine samples.

For the temperature calculations as if FTNP was pure calcite, using the equations from Coplen (2007) and Kim and O'Neil (1997), the temperatures calculated were 34.5 and 43 °C, respectively. The equation from Kele et al. (2015) gave a temperature of 47 °C, again higher than any

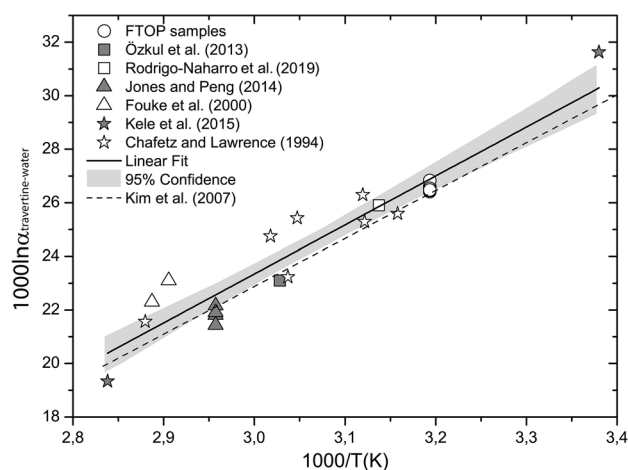


Fig. 6 $\delta^{18}\text{O}$ aragonite–water vs. $1000/T$ (in Kelvin). The natural aragonite samples previously identified as precipitated under an equilibrium situation are represented together with a linear fit. The 95% confidence interval of the fitting is also shown. Finally, the Kim et al. (2007) aragonite fractionation line is shown for comparison

possible water temperatures in the pipe, and this result was not considered.

The comparison of the results from these two samples indicate that: (1) the temperature range defined by the calculations from the aragonite travertines, FTOP, is quite narrow (36–40 °C) and perfectly coherent with the temperature of the parental water; (2) the temperature calculated from the calcite-rich travertine, FTNP, using the aragonite fractionation equations, is the same as the previous one, since their isotopic values are also the same; and (3) the temperature obtained using the calcite equations with the calcite-rich travertine (FTNP) gives a broader range, from 34.5 to 43 °C, that includes the two previous calculations with the aragonite calibration and also the range of the real waters circulating through the pipe (between 33 and 40 °C).

The $\delta^{18}\text{O}$ and temperature values of the studied aragonite travertines have been compared with those available in other natural aragonite samples precipitated under different conditions around the world, but always consisting of at least 90% of aragonite (Chafetz and Lawrence 1994; Fouke et al. 2000; Özkul et al. 2013; Jones and Peng 2014; Kele et al. 2015; Rodrigo-Naharro et al. 2019). As it is shown in Fig. 6, these data define a clear dependence on temperature that can be expressed as a $\delta^{18}\text{O}$ fractionation equation for natural aragonites in the temperature range of 23–80 °C (T is in Kelvin):

$$1000 \ln \alpha = 18.27(\pm 1.26) \times \frac{1000}{T} - 31.47(\pm 3.85); \quad (1)$$

this linear fit is represented in Fig. 6 together with the Kim et al. (2007) aragonite fractionation equation, which gives the most accurate temperature for the Fitero samples. It is remarkable that, despite the fact that the equation of Kim

et al. (2007) was calibrated with synthetic aragonites precipitated under controlled laboratory conditions, it is almost within the 95% of confidence of the fitting using the natural aragonite samples precipitated under different conditions and, most probably, with different precipitation rates. This result suggests that the main control in aragonite fractionation, in the examined samples, is the temperature and that equilibrium situations are not uncommon. The temperatures calculated using the proposed calibration (Eq. 1) are between 3 and 2.7 °C higher than the ones obtained with Kim et al.'s (2007) equation. In any case, the equation proposed here can be used as an additional tool to evaluate the natural aragonite isotope fractionation, although it should be improved with new isotope studies on aragonite samples.

Isotope equilibrium/disequilibrium and water temperature

It is usually considered that isotopic disequilibrium is the dominant condition during calcite and/or aragonite precipitation in travertine deposits due to kinetic effects induced by high CO₂ outgassing and high precipitation rates (e.g., Kele et al. 2008, 2011; Rodríguez-Berriguete et al. 2018 and references therein). Isotope-based temperature calculations require isotopic equilibrium and, therefore, disequilibrium situations would critically affect the accuracy of the temperature/paleotemperature calculations.

The fibrous-radial texture, the performed geochemical and mass balance calculations, and the carbon isotope compositions discussed in the previous sections, all suggest that disequilibrium conditions, associated with rapid CO₂ degassing and high precipitation rates, would prevail during the precipitation of the studied travertines. However, the δ¹⁸O values from the carbonates fall in the equilibrium window (Lachniet 2015) defined by the different δ¹⁸O aragonite/calcite-water fractionation equations proposed by different authors (Fig. 5), and the temperature calculated using those equations fits very well with the measured temperatures (in most cases within ± 3 °C or even better; Table 5).

Similar situations of successful temperature calculations despite the existence of isotopic disequilibrium conditions have been previously reported in the literature about calcite tufa deposits (e.g., Yan et al. 2012; Wang et al. 2014; Rodríguez-Berriguete et al. 2018) and they have been explained as due to the fact that the precipitated carbonates show an oxygen isotopic signal close to the one in the dissolved HCO₃⁻.

To check this possibility in the studied travertines, and following Kele et al. (2008, 2011), Halas and Wolacewicz (1982) equation ($1000 \ln \alpha_{\text{HCO}_3\text{-H}_2\text{O}} = 2.92 \cdot 10^6 / T^2 - 2.66$) was used to calculate the oxygen isotope fractionation between the dissolved HCO₃⁻ and the water at the temperatures of interest (between 33 and 40 °C) in the studied system. The values ranged between 27.11‰ at 40 °C and 28.4 ‰ at

33 °C. These values were compared with the ones measured for the oxygen fractionation between aragonite/calcite and water (as $1000 \ln \alpha_{\text{carbonate-H}_2\text{O}}$) which ranged from 26.42 to 26.63‰ considering both travertines (FTOP and FTNP).

These results indicate that for the precipitation temperature in the FTOP samples (40 °C, also representing the higher precipitation temperatures in the case of FTNP sample), the travertines show an oxygen isotopic signal close to that of the dissolved HCO₃⁻ suggesting an oxygen isotopic equilibrium between dissolved HCO₃⁻ and H₂O and a direct transfer of the HCO₃⁻ isotopic signal to the solids without fractionation. As stated by Kele et al. (2011), this absence of isotope fractionation can be promoted by fast CO₂ degassing and rapid carbonate precipitation (in agreement with the initial hypothesis by O'Neil et al. 1969), as it apparently occurs in the Fitero system.

This situation would explain the apparent equilibrium of the travertines with respect to the used δ¹⁸O aragonite/calcite–water fractionation equations. Furthermore, in agreement with other authors (Yan et al. 2012; Wang et al. 2014; Rodríguez-Berriguete et al. 2018), these results would suggest that some travertines can be used for paleotemperature calculations, even precipitating under disequilibrium conditions.

Conclusions

A mineralogical and isotopic characterisation of the Fitero aragonite travertines has been presented here. The parental water is the Fitero thermal water, which springs at 45 °C, although it is immediately cooled for its use in the spa. Two different travertine samples were studied: (1) one consisting of almost pure aragonite (98%), precipitated in a pipe which discharged water outside the cooling pool at a constant temperature of 40 °C; and (2) other composed of a mixture of 60% of calcite and 40% of aragonite taken in the general spa discharging pipe, where the water temperature varies between 33 and 40 °C. The precipitation of calcium carbonate is triggered by a CO₂ outgassing process (as deduced from the performed geochemical calculations and from the δ¹³C values calculated in the spring water and during travertines' precipitation) leading to the oversaturation of carbonate phases and, in turn, to the travertine precipitation. The main factor controlling aragonite or calcite precipitation in this system is the temperature, although the CO₂ loss can also play a role.

The evaluation of the δ¹⁸O values using different aragonite and calcite δ¹⁸O fractionation equations suggests that the precipitation of the Fitero travertines took place close to the isotope equilibrium, obtaining the most precise temperature with the equation proposed by Kim et al. (2007) for the aragonite fractionation. Non-significant differences between

aragonite–water and calcite–water fractionation have been found, since the $\delta^{18}\text{O}$ values in the aragonite samples and the mixture of calcite and aragonite sample are almost the same.

Given that in natural systems with important CO_2 outgassing rates, as in the case studied here, is unusual that the isotope equilibrium is maintained during precipitation, the possible reasons have been investigated. The most plausible explanation seems to be that the isotope signal of the dissolved HCO_3^- , in isotope equilibrium with water, is directly transferred to the precipitating carbonate, without fractionation, as a result of the quick CO_2 loss and precipitation. Therefore, under these apparent equilibrium situations, accurate temperature results could be expected using the $\delta^{18}\text{O}$ fractionation equations.

The temperature– $\delta^{18}\text{O}$ values of the aragonite deposits in Fitero have been compared with those in other natural aragonite travertines from the literature (always with aragonite proportions higher than 90%). Overall, they define a fractionation equation for natural aragonite in the temperature range of 23–80 °C, near the experimental equation of Kim et al. (2007), suggesting the existence of equilibrium, or apparent equilibrium, situations in an important number of natural travertine systems.

Acknowledgements M. Blasco has worked in this study thanks to a scholarship from the Ministry of Science, Innovation and Universities of Spain, for the Training of University Teachers (ref. FPU14/01523). This study forms part of the activities of the Geochemical Modelling Group (University of Zaragoza; Aragón Government). Authors would like to acknowledge the use of “Servicio General de Apoyo a la Investigación-SAI, Universidad de Zaragoza” and the technical assistance of Enrique Oliver from the Earth Sciences Department of the University of Zaragoza. The helpfulness of the Becquer Spa staff during the sampling is also grateful.

References

- AlKhatib M, Eisenhauer A (2017) Calcium and strontium isotope fractionation during precipitation from aqueous solutions as a function of temperature and reaction rate; II. Aragonite. *Geochim Cosmochim Acta* 209:320–342
- Andrews JE (2006) Palaeoclimatic records from stable isotopes in riverine tufas: synthesis and review. *Earth Sci Rev* 75:85–104
- Arenas C, Osácar MC, Auqué LF et al (2018) Seasonal temperatures from $\delta^{18}\text{O}$ in recent Spanish tufa stromatolites: equilibrium redux! *Sedimentology* 65:1611–1630
- Asta MP, Auqué LF, Sanz FJ et al (2017) Travertines associated with the Alhama-Jaraba thermal waters (NE, Spain): genesis and geochemistry. *Sediment Geol* 347:100–116
- Auqué LF, Fernández J, Tena Calvo JM (1988) Las aguas termales de Fitero (Navarra) y Arnedillo (Rioja). I. Análisis geoquímico de los estados de equilibrio-desequilibrio en las surgencias. *Estud Geol* 44:285–292
- Auqué LF, Fernández J, Tena Calvo JM et al (1989) Análisis de los estados de equilibrio termodinámico en el reservorio de las surgencias termales de Fitero (Navarra) y Arnedillo (Rioja). *Rev la Soc Geol Esp* 2:125–132
- Blasco M, Gimeno MJ, Auqué LF (2018) Low temperature geothermal systems in carbonate–evaporitic rocks: Mineral equilibria assumptions and geothermometrical calculations. Insights from the Arnedillo thermal waters (Spain). *Sci Total Environ* 615:526–539
- Blasco M, Auqué LF, Gimeno MJ (2019) Geochemical evolution of thermal waters in carbonate–evaporitic systems: the triggering effect of halite dissolution in the dedolomitisation and albitisation processes. *J Hydrol* 570:623–636
- Böhm F, Joachimski MM, Dullo WC et al (2000) Oxygen isotope fractionation in marine aragonite of coralline sponges. *Geochim Cosmochim Acta* 64:1695–1703
- Capezzuoli E, Gandin A, Pedley M (2014) Decoding tufa and travertine (fresh water carbonates) in the sedimentary record: the state of the art. *Sedimentology* 61:1–21
- Chacko T, Deines P (2008) Theoretical calculation of oxygen isotope fractionation factors in carbonate systems. *Geochim Cosmochim Acta* 72:3642–3660
- Chacko T, Cole DR, Horita J (2001) Equilibrium oxygen, hydrogen and carbon isotope fractionation factors applicable to geologic systems. *Rev Mineral Geochem* 43:1–81
- Chafetz HS, Lawrence JR (1994) Stable isotopic variability within modern travertines. *Géogr Phys Quat* 48:257–273
- Chafetz HS, Rush PF, Utech NM (1991) Microenvironmental controls on mineralogy and habit of CaCO_3 precipitates: an example from an active travertine system. *Sedimentology* 38:107–126
- Clark I, Fritz P (1997) Environmental isotopes in hydrogeology. CRC Press/Lewis Publishers, Boca-Raton (Florida)
- Coloma P (1998) El agua subterránea en La Rioja. *Zubía Monogr* 10:63–132
- Coloma P, Sánchez JA, Martínez FJ (1995) El drenaje subterráneo de la cordillera Ibérica en la depresión terciaria del Ebro (sector Riojano). *Geogaceta* 17:68–71
- Coloma P, Sánchez JA, Martínez FJ (1996) Procesos geotérmicos causados por la circulación del agua subterránea en el contacto entre la Sierra de Cameros y la Depresión Terciaria del Ebro. *Geogaceta* 20:749–753
- Coloma P, Sánchez JA, Martínez FJ (1997a) Sistemas de flujo subterráneo regional en el acuífero carbonatado mesozoico de la Sierra de Cameros. Sector Oriental. *Estud Geol* 53:159–172
- Coloma P, Sánchez JA, Martínez FJ, Pérez A (1997b) El drenaje subterráneo de la Cordillera Ibérica en la Depresión terciaria del Ebro. *Rev la Soc Geol Esp* 10:205–218
- Coloma P, Sánchez JA, Jorge JC (1998) Simulación matemática del flujo y transporte de calor del sector oriental de la Cuenca de Cameros. *Zubía Monogr* 10:45–61
- Coplen TB (2007) Calibration of the calcite-water oxygen-isotope geothermometer at Devils Hole, Nevada, a natural laboratory. *Geochim Cosmochim Acta* 71:3948–3957
- Craig H (1961) Isotopic variations in meteoric waters. *Science* 80(133):1702–1703
- Delgado A, Reyes E (2004) Isótopos estables como indicadores paleoclimáticos y paleohidrológicos en medios continentales. *Semin la Soc Española Mineral Geoquímica Isotópica Apl al Medioambiente* 1:37–53
- Demény A, Kele S, Siklós Z (2010) Empirical equations for the temperature dependence of calcite-water oxygen isotope fractionation from 10 to 70 °C. *Rapid Commun Mass Spectrom* 24:3521–3526
- Díaz-Teijeiro MF, Rodríguez-Arévalo J, Castaño S (2009) La Red Española de Vigilancia de Isótopos en la Precipitación (REVIP): distribución isotópica espacial y aportación al conocimiento del ciclo hidrológico. *Ing Civ* 155:87–97
- Fernández J, Auqué LF, Sánchez Cela VS, Guaras B (1988) Las aguas termales de Fitero (Navarra) y Arnedillo (Rioja). II. Análisis

- comparativo de la aplicación de técnicas geotermométricas químicas a aguas relacionadas con reservorios carbonatado-evaporíticos. *Estud Geol* 44:453–469
- Fischbeck R, Müller G (1971) Monohydrocalcite, hydromagnesite, nesquehonite, dolomite, aragonite and calcite in speleothems of the Frankische Schweiz, Western Germany. *Contrib Mineral Petrol* 33:87–92
- Folk RL (1994) Interaction between bacteria, nanobacteria, and mineral precipitation in hot springs of central Italy. *Géogr Phys Quat* 48:233–246
- Ford TD, Pedley HM (1996) A review of tufa and travertine deposits of the world. *Earth Sci Rev* 41:117–175
- Fouke BW, Farmer JD, Des Marais DJ et al (2000) Depositional facies and aqueous-solid geochemistry of travertine-depositing hot springs (Angel Terrace, Mammoth Hot Springs, Yellowstone National Park, U.S.A.). *J Sediment Res* 70:565–585
- Friedman I (1970) Some investigations of the deposition of travertine from Hot Springs-I. The isotopic chemistry of a travertine-depositing spring. *Geochim Cosmochim Acta* 34:1303–1315
- Friedman I, O'Neil JR (1977) Compilation of stable isotope fractionation factors of geochemical interest. In: Fleischer M (ed) *Data on geochemistry*, USGS professional paper 440-KK, 6th edn. United States Government Printing Office, Washington, p 109
- Gabitov RI (2013) Growth-rate induced disequilibrium of oxygen isotopes in aragonite: an in situ study. *Chem Geol* 351:268–275
- Garnett ER, Andrews JE, Preece RC, Dennis PF (2004) Climatic change recorded by stable isotopes and trace elements in a British Holocene tufa. *J Quat Sci* 19:251–262
- Gil A, Villalain JJ, Barbero L et al (2002) Aplicación de Técnicas geoquímicas, geofísicas y mineralógicas al estudio de la Cuenca de Cameros. *Implicaciones Geométricas y Evolutivas Zubía Monográfico* 14:65–98
- Goy A, Gómez JJ, Yébenes A (1976) El Jurásico de la Rama Castellana de la Cordillera Ibérica (Mitad norte) I. Unidades litoestratigráficas. *Estud Geol* 32:391–423
- Grossman EL, Ku T (1986) Oxygen and carbon isotope fractionation in biogenic aragonite: temperature effects. *Chem Geol* 59:59–74
- Halas S, Wolaciewicz W (1982) The experimental study of oxygen isotope exchange reaction between dissolved bicarbonate and water. *J Chem Phys* 76:5470–5472
- Horita J, Clayton RN (2007) Comment on the studies of oxygen isotope fractionation between calcium carbonates and water at low temperatures by Zhou and Zheng (2003; 2005). *Geochim Cosmochim Acta* 71:3131–3135
- Jones B (2017a) Review of aragonite and calcite crystal morphogenesis in thermal spring systems. *Sediment Geol* 354:9–23
- Jones B (2017b) Review of calcium carbonate polymorph precipitation in spring systems. *Sediment Geol* 353:64–75
- Jones B, Peng X (2014) Hot spring deposits on a cliff face: a case study from Jifei, Yunnan Province, China. *Sediment Geol* 302:1–28
- Jones B, Peng X (2016) Mineralogical, crystallographic, and isotopic constraints on the precipitation of aragonite and calcite at Shiqiang and other hot springs in Yunnan Province, China. *Sediment Geol* 345:103–125
- Jones B, Renaut RW (1995) Noncrystallographic cendrites from hot-spring deposits at Lake Bogoria, Kenya. *J Sediment Res* A65:154–169
- Jones B, Renaut RW (2010) Calcareous spring deposits in continental settings. In: Alonso-Zarza AM, Tanner LH (eds) *Developments in sedimentology: carbonates in continental settings: facies, environments and processes*. Elsevier, Amsterdam, pp 177–224
- Jones B, Renaut RW, Rosen MR (1996) High-temperature ($\approx 90^\circ\text{C}$) calcite precipitation at Waikite Hot Springs, North Island, New Zealand. *J Geol Soc Lond* 153:481–496
- Kele S, Demény A, Siklósy Z et al (2008) Chemical and stable isotope composition of recent hot-water travertines and associated thermal waters, from Egerszalók, Hungary: depositional facies and non-equilibrium fractionation. *Sediment Geol* 211:53–72
- Kele S, Özkul M, Fórizs I et al (2011) Stable isotope geochemical study of Pamukkale travertines: new evidences of low-temperature non-equilibrium calcite-water fractionation. *Sediment Geol* 238:191–212
- Kele S, Breitenbach SF, Capezzuoli E et al (2015) Temperature dependence of oxygen- and clumped isotope fractionation in carbonates: a study of travertines and tufas in the 6–95 °C temperature range. *Geochim Cosmochim Acta* 168:172–192
- Kim ST, O'Neil JR (1997) Equilibrium and nonequilibrium oxygen isotope effects in synthetic carbonates. *Geochim Cosmochim Acta* 61:3461–3475
- Kim ST, O'Neil JR (2005) Comment on “An experimental study of oxygen isotope fractionation between inorganically precipitated aragonite and water at low temperatures” by G.-T. Zhou and Y.-F. Zheng. *Geochim Cosmochim Acta* 69:3195–3197
- Kim S-T, O'Neil JR, Hillaire-marcel C et al (2007) Oxygen isotope fractionation between synthetic aragonite and water. Influence of temperature and Mg^{2+} concentrations. *Geochim Cosmochim Acta* 71:4704–4715
- Kitano Y (1963) Geochemistry of calcareous deposits found in hot springs. *J Earth Sci* 11:68–100
- Lachniet MS (2015) Are aragonite stalagmites reliable paleoclimate proxies? Tests for oxygen isotope time-series replication and equilibrium. *GSA Bull* 1521–1533
- Lachniet MS, Bernal JP, Asmerom Y et al (2012) A 2400-yr Mesozoic rainfall history links climate and cultural change in Mexico. *Geology* 40:259–262
- Last WM (1989) Continental brines and evaporites of the northern Great Plains of Canada. *Sediment Geol* 64:207–221
- Last WM, Vance RE, Wilson S, Smol JP (1998) A multi-proxy limnologic record of rapid early-Holocene hydrologic change on the northern Great Plains, southwestern Saskatchewan, Canada. *Holocene* 8:503–520
- Lécuyer C, Hutzler A, Amiot R et al (2012) Carbon and oxygen isotope fractionations between aragonite and calcite of shells from modern molluscs. *Chem Geol* 332–333:92–101
- Li HC, Lee ZH, Wan NJ et al (2011) The $\delta^{18}\text{O}$ and $\delta^{13}\text{C}$ records in an aragonite stalagmite from Furong Cave, Chongqing, China: A-2000-year record of monsoonal climate. *J Asian Earth Sci* 40:1121–1130
- Li TY, Shen CC, Li HC et al (2012) Oxygen and carbon isotopic systematics of aragonite speleothems and water in Furong Cave, Chongqing, China. *Geochim Cosmochim Acta* 75:4140–4156
- Liu Z, Li H, You C et al (2006) Thickness and stable isotopic characteristics of modern seasonal climate-controlled sub-annual travertine laminae in a travertine-depositing stream at Baishuitai, SW China: implications for paleoclimate reconstruction. *Environ Geol* 51:257–265
- Liu Z, Sun H, Baoying L et al (2010) Wet-dry seasonal variations of hydrochemistry and carbonate precipitation rates in a travertine-depositing canal at Baishuitai, Yunnan, SW China: implications for the formation of biannual laminae in travertine and for climatic reconstruction. *Chem Geol* 273:258–266
- Lojen S, Dolenc T, Vokal B et al (2004) C and O stable isotope variability in recent freshwater carbonates (River Krka, Croatia). *Sedimentology* 51:361–375
- Lojen S, Trkov A, Ščančar J et al (2009) Continuous 60-year stable isotopic and earth-alkali element records in a modern laminated tufa (Jaruga, river Krka, Croatia): implications for climate reconstruction. *Chem Geol* 258:242–250
- Mas JR, Alonso A, Guimera J (1993) Evolución tectonosedimentaria de una cuenca extensional intraplaca: la cuenca

- finijurásica-eocretácica de los Cameros (La Rioja-Soria). *Rev Soc Geol Esp* 6:129–144
- McCrea JM (1950) On the isotopic chemistry of carbonates and a paleotemperature scale. *J Chem Phys* 18:849–857
- Minissale A (2004) Origin, transport and discharge of CO₂ in central Italy. *Earth-Sci Rev* 66:89–141
- Mook WG, Bommerson JC, Staverman WH (1974) Carbon isotope fractionation between dissolved bicarbonate and gaseous carbon dioxide. *Earth Planet Sci Lett* 22:169–176
- O'Neil JR, Clayton RN, Mayeda TK (1969) Oxygen isotope fractionation in divalent metal carbonates. *J Chem Phys* 51:5547–5558
- Osácar C, Arenas C, Vázquez-Urbez M et al (2013) Environmental factors controlling the $\delta^{13}\text{C}$ and $\delta^{18}\text{O}$ variations of recent fluvial tufas: a 12-year record from the monasterio de piedra natural park (NE Iberian Peninsula). *Sediment Geol* 83:309–322
- Osácar C, Arenas C, Auqué LF et al (2016) Discerning the interactions between environmental parameters reflected in $\delta^{13}\text{C}$ and $\delta^{18}\text{O}$ of recent fluvial tufas: lessons from a Mediterranean climate region. *Sediment Geol* 345:126–144
- Özkul M, Kele S, Gökğöz A et al (2013) Comparison of the Quaternary travertine sites in the Denizli extensional basin based on their depositional and geochemical data. *Sediment Geol* 294:179–204
- Panichi C, Tongiorgi E (1976) Carbon isotopic composition of CO₂ from springs, fumaroles, mofettes and travertines of central and southern Italy: a preliminary prospection method of geothermal areas. In: *Proceedings 2nd U.N. Symposium on the Development and Use of Geothermal Energy*, San Francisco. pp 815–825
- Parkhurst DL, Appelo CAJ (2013) Description of Input and Examples for PHREEQC Version 3. A Computer Program for Speciation, Batch Reaction, One Dimensional Transport, and Inverse Geochemical Calculations. In: *U.S. Geological Survey (ed) Techniques and Methods*, book 6, chap. A43. U.S. Geological Survey, Denver, Colorado
- Patterson WP, Smith GR, Lohmann KC, Kyger CL (1993) Continental Paleothermometry And Seasonality Using The Isotopic Composition Of Aragonitic Otoliths Of Freshwater Fishes. In: Swart PK, Lohmann KC, McKenzie J, Savin S (eds) *Climate change in continental isotopic records*. American Geophysical Union, pp 191–202
- Pedley M (2009) Tufas and travertines of the Mediterranean region: a testing ground for freshwater carbonate concepts and developments. *Sedimentology* 56:221–246
- Peng X, Jones B (2012) Rapid precipitation of silica (opal-A) disguises evidence of biogenicity in high-temperature geothermal deposits: case study from Dagunguo hot spring, China. *Sediment Geol* 257–258:45–62
- Pentecost A (2005) *Travertine*. Springer Science & Business Media
- Reyes E, Pérez del Villar L, Delgado A et al (1998) Carbonation processes at the El Berrocal analogue granitic systema (Spain): mineralogical and isotopic study. *Chem Geol* 150:293–315
- Rietveld HM (1969) A profile refinement method for nuclear and magnetic structures. *J Appl Crystallogr* 2:65–71
- Rodrigo-Naharro J, Herrero MJ, Delgado-Huertas A et al (2019) Current travertines precipitation related to artificial CO₂ leakages from a natural reservoir (Gañuelas-Mazarrón Tertiary Basin, SE Spain). *J Hydrol* 577:123997
- Rodríguez-Berriguete Á, Alonso-Zarza AM, Martín-García R, del Cabrera MC (2018) Sedimentology and geochemistry of a human-induced tufa deposit: Implications for palaeoclimatic research. *Sedimentology* 65:2253–2277
- Romanek CS, Grossman EL, Morse JW (1992) Carbon isotopic fractionation in synthetic aragonite and calcite: effects of temperature and precipitation rate. *Geochim Cosmochim Acta* 56:419–430
- Sánchez JA, Coloma P (1998) *Hidrogeología de los manantiales termales de Arnedillo*. Zubía Monogr 10:11–25
- Scheele N, Hoefs J (1992) Carbon isotope fractionation between calcite, graphite and CO₂: an experimental study. *Contrib Mineral Petrol* 112:35–45
- Sierralta M, Kele S, Melcher F et al (2010) Uranium-series dating of travertine from Süttő: implications for reconstruction of environmental change in Hungary. *Quat Int* 222:178–193
- Szaran J (1997) Achievement of carbon isotope equilibrium in the system HCO₃⁻ (solution)-CO₂ (gas). *Chem Geol* 142:79–86
- Thorrold SR, Campana SE, Jones CM, Swart PK (1997) Factors determining $\delta^{13}\text{C}$ and $\delta^{18}\text{O}$ fractionation in aragonitic otoliths of marine fractionation in aragonitic otoliths of marine fish. *Pergamon Geochim Cosmochim Acta* 61:2909–2919
- Turner JV (1982) Kinetic fractionation of carbon-13 during calcium carbonate precipitation. *Geochim Cosmochim Acta* 46:1183–1191
- Wang Z, Gaetani G, Liu C, Cohen A (2013) Oxygen isotope fractionation between aragonite and seawater: developing a novel kinetic oxygen isotope fractionation model. *Geochim Cosmochim Acta* 117:232–251
- Wang H, Yan Y, Liu Z (2014) Contrasts in variations of the carbon and oxygen isotopic composition of travertines formed in pools and a ramp stream at Huanglong Ravine, China: implications for paleoclimatic interpretations. *Geochim Cosmochim Acta* 125:34–48
- Wassenburg JA, Scholz D, Jochum KP et al (2016) Determination of aragonite trace element distribution coefficients from speleothem calcite–aragonite transitions. *Geochim Cosmochim Acta* 190:347–367
- White RMP, Dennis PF, Atkinson TC (1999) Experimental calibration and field investigation of the oxygen isotopic fractionation between biogenic aragonite and water. *Rapid Commun Mass Spectrom* 13:1242–1247
- Yan H, Sun H, Liu Z (2012) Equilibrium vs. kinetic fractionation of oxygen isotopes in two low-temperature travertine-depositing systems with differing hydrodynamic conditions at Baishuitai, Yunnan SW China. *Geochim Cosmochim Acta* 95:63–78
- Zavdlav S, Rozic B, Dolenc M, Lojen S (2017) Stable isotopic and elemental characteristics of recent tufa from a karstic Krka River (south-east Slovenia): useful environmental proxies? *Sedimentology* 64:808–831
- Zhang J, Quay PD, Wilbur DO (1995) Carbon isotope fractionation during gas-water exchange and dissolution of CO₂. *Geochim Cosmochim Acta* 59:107–114
- Zheng YF (1999) Oxygen isotope fractionation in carbonate and sulfate minerals. *Geochem J* 33:109–126
- Zheng YF (2011) On the theoretical calculations of oxygen isotope fractionation factors for carbonate-water systems. *Geochem J* 45:341–354
- Zhou G-T, Zheng Y-F (2003) An experimental study of oxygen isotope fractionation between inorganically precipitated aragonite and water at low temperatures. *Geochim Cosmochim Acta* 67:387–399